

Omni-supervised Facial Expression Recognition: A Simple Baseline

Ping Liu, Yunchao Wei, Zibo Meng, Weihong Deng, Joey Tianyi Zhou, and Yi Yang

Abstract—The performance of the current state-of-the-art FER approaches usually degrades on unseen data in-the-wild because the training datasets are generally collected under well-controlled settings, and the number of labeled training samples is normally limited. To enhance the robustness of the deep models for facial expression recognition in various scenarios, in this paper, we propose to perform omni-supervised learning by exploiting not only the labeled samples, but also the unlabeled data, which is relatively easy to obtain and can introduce more variations to improve the generality of the trained model. Particularly, first, a primitive model trained on a small number of labeled samples is adopted to select samples with high confidence scores from a facial-pool, *i.e.*, MS-Celeb-1M, according to feature-based similarity comparison. Then we notice that the new dataset constructed in such an omni-supervised manner can significantly improve the generalization ability of the learned FER model and boost the performance consequently. However, as more training samples are used, more computational resources and training time are required, which is usually not affordable in many circumstances. To alleviate the requirement of computational resources, we further propose to deploy the dataset distillation strategy to distill the target task-related knowledge from the new mined samples and compressed them into a very small set of images. This distilled dataset is capable of boosting the performance of FER with few additional computational costs introduced. We perform extensive experiments on popular benchmarks, where consistent gains can be achieved under various settings using the proposed framework. We hope this work will serve as a solid baseline and help ease future research in FER.

Index Terms—Facial Expression Recognition, Omni-supervised Learning, Dataset Distillation, Cross-dataset Evaluation.

1 INTRODUCTION

Facial activity, as one of the most important emotion and intention sensing cues for humans, has been extensively studied in the past decades. A robust system for facial activity analysis should be able to recognize the basic expressions [1], *i.e.*, anger, disgust, fear, happy, sad, surprise, and/or compound expressions from facial images. With the development in human-computer interaction, a highly accurate and efficient facial expression recognition (FER) system is desired in various real scenarios, such as remote education, online entertainment, and intelligent autonomous transportation.

Before the emerging of deep learning methods, researchers have designed various hand-crafted features such as local binary patterns (LBP), histogram of gradient (HoG), and scale invariant feature transform (SIFT) to model the appearance and geometry changes of expressive faces [2], [3], [4], [5], [6], [7], [8], [9], [10]. Comparing to previous works based on hand-crafted features, convolutional neural networks (CNNs) based methods for FER have brought about significant performance improvements [11], [12], [13]. However, to train a robust deep network for a specific task, a huge amount of labeled data with high quality is required. Nonetheless, in FER, existing publicly available datasets [1], [14], [15] are generally constructed under controlled lab experiments with a limited number of samples. In a con-

trolled environment, the variations introduced by different factors, *e.g.*, head poses, light conditions, and etc. can be limited and fails to represent the real scenarios. Thus, the facial expression data collected in a lab controlled setting is significantly different from the facial expression data collected in the wild. This well-known “domain shift” issue deteriorates the generality of the trained FER model [16]. More than that, due to the privacy concerns, collecting facial expression data in a lab controlled environment is labor expensive and time-consuming, which lessen the facial expression datasets collected to a small size (thousands [1] or even hundreds [15]).

Inspired by the progress of semi-supervised learning and unsupervised learning, researchers on facial expression recognition resort their eyes to the huge amounts of facial images from Internet in order to solve the data shortage problem has been bothering them. However, how to take advantage of those huge-scale data as well as the labeled small size data is still under exploration. One plausible way to make full use of those huge-scale data, is to utilize them to conduct unsupervised learning, *e.g.*, pre-train the network [16] to provide a good initialization for the *following* finetune step. We argue that an alternative, and (maybe) better way is to perform semi/omni-supervised learning by exploiting the current labeled data *together* with large-scale unlabeled data to train the network. As pointed out by [17], the performance of an omni-supervised learner, which utilizes both large-scale unlabeled data and the small size labeled data, can outperform its counterpart utilizing labeled data alone.

In this work, we propose a simple yet effective omni-supervised baseline for facial expression recognition, where we exploit the useful knowledge from a large-scale *unlabeled*

- P. Liu, Joey Zhou are with Institute of High Performance Computing, Agency for Science, Technology, and Research, Singapore.
- Y. Wei, Y. Yang are with Centre for Artificial Intelligence, University of Technology Sydney, Sydney, Australia.
- W. Deng is with Pattern Recognition and Intelligent System Laboratory, Beijing University of Posts and Telecommunications, Beijing, China.
- Z. Meng is with InnoPeak Technology Inc., Palo Alto, USA.

Manuscript received April 19, 2005; revised August 26, 2015.

dataset to improve the performance of the facial expression learner. Under the omni-supervised learning setting, we annotate those unlabeled data in an *automatic* manner. After discarding unaccountable samples, which might bring the noise to training, a huge scale labeled data (near to 140K) with fine quality is constructed. Taking advantage of this constructed dataset as well as the *manually* labeled training set for training can greatly boost the recognition accuracy of the testing set, which has been proved by our experimental results.

Although the newly constructed dataset can significantly improve the performance of FER, it also brings some new issues. First, the size of our constructed dataset is significantly large (hundreds of thousands), making the training time-consuming and computation resource exhausted. Thus, it may not be affordable by those research groups with limited computation resources. Second, since the constructed dataset is annotated automatically without human interventions, there might still exist some incorrectly labeled samples, which may bring noisy information. Third, the sample number of each class in the constructed dataset are not balanced, which might bring unexpected bias for training. To tackle the above-mentioned issues, we propose to utilize the dataset distillation strategy [18] to distill the target task-related knowledge from the constructed dataset and compress them into a small set of images (in our case, one image represents one single category). Comparing to the vanilla collected dataset in large sizes, the computational cost introduced by the distilled version for FER learner training can be almost ignored. Although with a small size, this distilled dataset is still capable of boosting the recognition accuracy to a higher stage in both inner-dataset evaluation and cross-dataset evaluation, which has been demonstrated in our experiment.

In general, we list our main contributions in this work as follows:

- We construct a large-scale dataset and exploit it for omni-supervised facial expression recognition, aiming to boost the recognition accuracy. Unlike previous works utilizing an unlabeled dataset for pre-train the network and provide initialization for downstream fine-tuning, our method employs omni-supervised learning setting by taking advantage of the constructed huge-scale dataset as well as the small size labeled dataset to strengthen the FER learner.
- To improve the generality, decrease the training cost, and balance the class ratios, we propose to utilize the dataset distillation strategy to summarize the knowledge from the constructed dataset. Specifically, by the dataset distillation strategy, the constructed dataset, which has around 140K images, is compressed into a significant small image set, in which one image for each class. The highly summarized knowledge in the distilled small set can be exploited together with the small size manually labeled data to improve the generality power of the FER learner.
- We conduct extensive experiments on FER benchmarks, demonstrating the superiority of the simple yet effective baseline method. We also conduct cross-

dataset evaluations, *i.e.*, training a CNN on a source dataset but test on a different target dataset, which is quite challenging due to the well-known “domain-shift” issues. Our performances in this cross-data setting demonstrate the superior generality of the proposed method.

2 RELATED WORK

This section will focus on facial expression recognition and omni-supervised learning, which are the most related topics with this article.

2.1 Facial Expression Recognition

With the development of modern convolutional neural networks, various deep learning methods have been applied to facial expression recognition problems. Recent works based on deep learning methods [11], [12], [13], [19], [20], [21] outperform their counterparts without using deep learning [2], [3], [4], [5], [6], [7], [8], [9], [10], [22], [23], [24], [25]. [19] proposes to unify Deep Belief Network and Boosting methods to perform feature learning, feature selection, and classifier construction in a joint way. [20] constructs an Inception-wise network and achieves promising recognition rates on seven public facial expression databases. For focusing on variations introduced by expressions, [11], [12], [13] propose to disentangle expression-sensitive knowledge and analyze the facial expressions based on the expression-sensitive knowledge. To suppress the variations introduced by different identities, [11] proposes an identity-aware convolutional neural network to differentiate the identity sensitive knowledge from expression sensitive knowledge. [12] proposes to utilize generative adversarial networks (GANs) to disentangle expression variations from pose variations. [13] proposes to extract facial expressive information by a designed de-expression module. To recognize facial expressions in various unconstrained conditions, [21] proposes to utilize attention mechanisms in CNNs and [26] utilizes a privileged learning mechanism to adjust the importance of feature learned from different facial regions. Interested readers can read [27] for a systematic review of deep facial expression recognition works.

2.2 Semi/Omni-supervised Learning

A successful CNN based feature learning process is heavily dependent on large scale training data with high-quality labels. Unfortunately, manually labeling huge amounts of data in high quality is time-consuming and labor-expensive. To deal with this limitation, semi-supervised learning [17], [28], [29], [30], [31], [32] is utilized to improve final performance. Among those previous works, [32] follows a strategy that has been proved effective in previous works: introduce huge scale unlabeled data to pretrain the network, provide a good initialization for the downstream finetuning process. However, there are a few limitations in this strategy [32]. Introduce huge-scale unlabeled data to pretrain the network occupies additional computation resources and time. More than that, the domain gap existing between the unlabeled data used for pretraining and labeled data used for finetuning, might bring unexpected bias during the

training process. On the contrary, our method is based on omni-supervised learning, combining a huge-scale dataset constructed automatically by our method with a small size labeled dataset. In our method, the constructed dataset participates in the FER learner training process, rather than acting as an initializer. This is because our method managed to minimize the gap between the constructed dataset in a large scale and the small size labeled dataset.

3 METHODOLOGY

In this section, we illustrate the details of the proposed method step by step. As shown in Fig. 1, first, we utilize the labeled data in a small size to train a primitive classifier (Sec. 3.2). Second, this primitive classifier is then utilized to provide guidance to select the most confident unlabeled data from large-scale sets (Sec. 3.3). Specifically, unlike previous works choosing the confident samples based on their category likelihood, this proposed baseline method is based on the similarity between high-level features extracted from the layer before the softmax output layer. Those huge scale selected samples are constructed into a new dataset, which will collaborate with the original small size labeled dataset to strengthen the network. Further, to decrease the computation cost, save the training time, and increase the generality of the network, we propose to utilize the dataset distillation strategy to compress the huge-scale constructed dataset into a very small set, in which one image for one class (Sec. 3.4).

3.1 Task Definition

Facial expression recognition aims to learn a mapping function to map the original input image x to a latent representation. This latent representation should have the discriminative capability to distinguish samples from different classes. In this article, the mapping process is conducted by a convolutional neural network (CNN), which is denoted as $f(\cdot; \theta)$ and learned by labeled data $\{x_i^l, y_i^l\}, 1 \leq i \leq N$. The learning formulation is as follows:

$$\min \sum_{i=1}^N L(W * f(x_i; \theta), y_i) \quad (1)$$

where $L(\cdot, \cdot)$ is the loss function, W is the classifier parameter, θ is the CNN parameter.

In this work, we target to improve the generality of the learned network $f(\cdot; \theta)$ by constructing a large scale dataset and apply it under the omni-supervised learning setting.

3.2 Primitive Learner Training on Labeled Data

As shown in Figure. 1 (a), in the first step, we utilize labeled data on hand, *i.e.*, $\{x_i^l, y_i^l\}$, to train a primitive learner $f(\cdot; \theta)$, where θ denotes model parameters. To make the following discussion convenient, we name the utilized manually labeled dataset as the anchor data. Given an input x_i^l , the trained primitive learner needs to predict the correct label y_i^l . Our method is model-agnostic, and we can choose any architectures that have demonstrated their effectiveness for visual recognition problems [33], [34], [35], [36]. We do not need to modify the chosen architecture or introduce any new loss terms to achieve better performance. The only

replacement we need is to replace the final classifier layers and change the output number to the number of target facial expression classes. In this article, the output number is set to 7 since there are seven basic facial expressions to detect, *i.e.*, anger, happy, disgust, fear, sad, surprise, and neutral. In this step, the primitive learner is trained only via annotated facial expression data, which is in a limit size due to collection and annotation cost.

3.3 Auxiliary Samples Collection from Unlabeled Data

This work targets to improving the recognition power of the FER learner by using the knowledge from huge-scale unlabeled data, which is denoted as $\{x_i^{ul}, y_i^{ul}\}$. The adopted approach in this work is to select huge scale samples from the unlabeled data. To make the FER learner benefit from the selected unlabeled samples, the selected data should share similar statistical distributions with the labeled ones, by which the domain gap problem can be alleviated to the most. Concretely, for each unlabelled data x_i^{ul} , we feed it to the primitive learner $f(\cdot; \theta)$ to generate its latent features $f(x_i^{ul}; \theta)$ and corresponding class confidence score by the following formulation:

$$P(y_i|f(x_i^{ul}; \theta)) = \frac{\exp(\mathbf{w}_i^T f(x_i^{ul}; \theta))}{\sum_{j=1}^m \exp(\mathbf{w}_j^T f(x_i^{ul}; \theta))}, \quad (2)$$

where \mathbf{w}_j is the weight vector for the j -th class, m is the number of classes. In our experiment, m is set as 7.

How to choose the appropriate samples sharing similar statistical distribution with labeled data from the image pool? One possible way is to utilize the probability score calculated by a pre-trained learner for the selection. Utilizing unlabeled data with pseudo labels generated by probability scores to update the original network has been explored in previous works on semi-supervised learning [28] and unsupervised learning [37]. However, in FER, the labeled data and unlabeled data are usually collected in different environments for different target tasks, which makes the conditional distributions between those databases different. The phenomenon is known as “domain shift”, which has been noticed and studied in previous works [16]. As pointed out by [16], in such cases, the generated probability scores and corresponding pseudo-labels for the unlabeled data, might be error-prone, and consequently it might mislead the network learning process if choose the unlabeled samples by their confidence score.

As concluded in [38], for samples x_i in the same class, the corresponding learned latent features $f(x_i^{ul}; \theta)$ have a tendency to cluster together. The dimension of $f(x_i^{ul}; \theta)$ is usually much higher than that of probability score $P(\cdot, \cdot)$, which makes them more robust in learning processes. Therefore, we follow the similar strategy in [38] to select *clean* and *related* samples from the unlabeled data under the guidance provided by manually labeled data.

Following the same strategy, we feed each labeled sample x_i^l into the primitive network $f(\cdot; \theta)$ to calculate its latent feature representation $f(x_i^l; \theta)$. Since we have the ground truth for those labeled data, we can calculate the

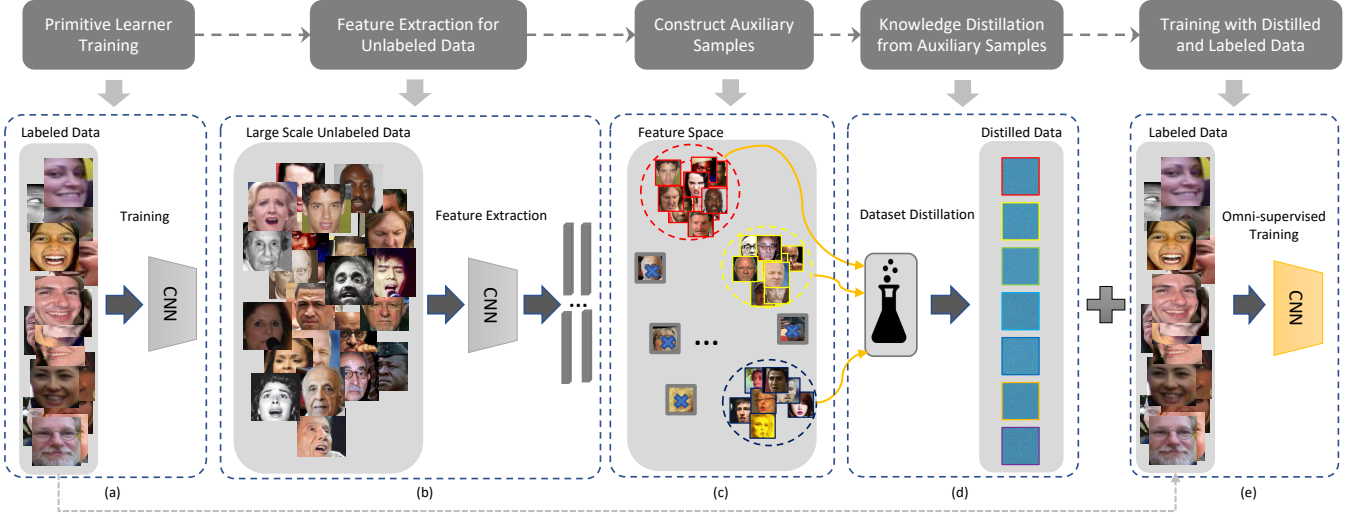


Fig. 1. An illustration for the whole pipeline. First, we utilize labeled data on hand to train a primitive classifier. Since the labeled dataset for FER is often with a small size, the computation cost in this step is not huge and acceptable. Second, this primitive classifier will be utilized to provide guidance to select the most related unlabeled data from large-scale sets. Specifically, unlike previous works choosing the related samples based on their category likelihood, this proposed baseline method is based on high-level features with semantic meaning, which is extracted by the utilized primitive classifier. Knowledge related to FER will be injected into the training process, in which the useful information from unlabeled data and labeled data both contribute to the network training. Since the unlabeled data set probably consists of huge amounts of data, we utilize dataset distillation strategy [18] to compress the knowledge into a highly refined set, *i.e.*, one image for each class in our case. This highly distilled knowledge from huge-scale unlabeled data will be combined with the original labeled data together to train a stronger FER learner.

centroid in the feature space for each class, by the following formulation:

$$center_k = \frac{\sum_i \Delta(y_i^l == k) \times f(x_i^l; \theta)}{\sum_i \Delta(y_i^l == k)}, \quad (3)$$

where $\Delta(x)$ is 1 when x is true, k is the class index for basic facial expressions.

As shown in Figure 1 (b) and (c), for each unlabeled data sample x_i^{ul} , we also input it into the primitive network to produce its feature representation $f(x_i^{ul}; \theta)$, and then compute the distance between the calculated $f(x_i^{ul}; \theta)$ and each facial expression centorids, *i.e.*, $center_k$. In this work, we utilize the cosine distance with the following formulation:

$$d(center_k, f_i) = \frac{center_k \cdot f(x_i^l; \theta)}{\|center_k\| \|f(x_i^l; \theta)\|} \quad (4)$$

Then, we set the pseudo label for each unlabeled sample based on the following criterion:

$$y_i^{ul} = \hat{k}, \text{if } d(center_{\hat{k}}, f_i) \leq d(center_k, f_i) - \delta, \forall k \neq \hat{k} \quad (5)$$

where k is the class index for the facial expressions, δ is a margin threshold.

Our hypothesis is that generated pseudo labels based on high dimensional features are more robust and less error-prone. The selected unlabeled samples based on the pseudo labels share the similar statistical distribution with the labeled samples. Those selected samples from the unlabeled database will be combined with those from the labeled database to update the model. To make the following discussion simple, we name those selected samples from an unlabeled database by our method as auxiliary samples. In our experiment, the number of auxiliary samples selected from the unlabeled MS1M-Celeb-1M (MS1M for short) is 137,769. We show examples of selected auxiliary samples in

Algorithm 1 Algorithm Description of Dataset Distillation [18]

Input: the selected auxiliary samples with size N ; n : the distilled sample number; $p(\theta)$: distribution of initial network weights; η_0 : initialization for η ; α : step size; M : batch size; T : the iteration number;

1: **Initialize:** $\tilde{\mathbf{x}} = \{\tilde{x}_i\}_{i=1}^n, \eta = \eta_0$
 2: **for** $t = 1; t \leq T; t + +$ **do**
 3: fetch the current batch data $\mathbf{x}_t = \{x_{t,j}\}_{j=1}^M$
 4: sample a batch of initial weights θ_0^j based on distribution $p(\theta_0)$
 5: **for** each sampled θ_0^j **do**
 6: $\theta_1^j = \theta_0^j - \eta \nabla_{\theta_0^j} l(\tilde{\mathbf{x}}, \theta_0^j)$
 7: $L^j = l(\mathbf{x}_t, \theta_1^j)$
 8: **end for**
 9: Update: $\tilde{\mathbf{x}} = \tilde{\mathbf{x}} - \alpha \nabla_{\tilde{\mathbf{x}}} \sum_j L^j, \eta = \eta - \alpha \nabla_{\eta} \sum_j L^j$
 10: **end for**

Output: distilled data $\tilde{\mathbf{x}}$

Figure 3, in which selected samples are sorted by their distance values to corresponding class centroids.. The selected auxiliary samples collaborate with the manually labeled data by feeding to the primitive FER learner $f(\cdot; \theta)$ to refine the parameter θ and the classifier parameter W .

3.4 Knowledge Distillation from Auxiliary Samples

The auxiliary samples provided by the internet-scale unlabeled dataset to improve the recognition performance are demonstrated in our experimental results, which will be discussed in Section 4.4.1 and 4.4.2. However, the number of the selected auxiliary samples can be huge, which is 137,769 in this work. And this number might keep increasing if we continue introducing more unlabeled data samples grabbed

from the internet. Directly utilize the huge number of auxiliary samples selected to refine the FER learner becomes computationally expensive. Other than that, it is inevitable that some noisy samples still exist in those selected unlabeled data, although we choose the strategy mentioned in the last subsection. Therefore, further efforts are required to minimize the computation cost and noisy information brought by the auxiliary samples while maintaining the knowledge existing among those auxiliary samples as much as possible.

To solve the above mentioned problem, as shown in Fig. 1 (d), we deploy dataset distillation [18]. Unlike model distillation, which distills knowledge from a set of separately trained learners into a compact one, dataset distillation conducts an orthogonal task: keep the learner fixed while distill the knowledge existing in a whole dataset and compress them into a sparse set of synthetic images. By an elegantly designed algorithm [18], the distilled image set, although with a small size, has the capability to achieve the same or comparable performance if used for training the target network.

Assume we have selected N auxiliary samples, and we would like to encapsulate the knowledge in those N samples into n distilled samples, where $n \ll N$. By conducting the dataset distillation algorithm illustrated in Algorithm 1, which is cited from [18], we distill the knowledge from the huge size of auxiliary samples into a small set of synthetic images, denoted as \tilde{x} . We utilize the generated \tilde{x} as well as the labeling dataset in small sizes to refine our FER learner, which will also improve the FER learner capability with much less computation cost in training.

In summary, utilize the distilled auxiliary samples rather than the vanilla auxiliary samples in a huge size has three advantages: 1). the distilled images are with a small size, introducing few computation cost; 2) comparing to the vanilla auxiliary collected samples, the distilled images are with high generality capability, which has been experimentally proved to benefit to the cross-dataset evaluation settings; 3) the sample number of each class in distilled auxiliary data is balanced, without the potential of hurting the data balance when training.

4 EXPERIMENTAL RESULTS

This section evaluates the performance of the proposed method to demonstrate its effectiveness. First, an inner-database evaluation on two in-the-wild datasets is conducted to demonstrate the efficacy of our large-scale collected dataset as well as the distilled version; second, a cross-database evaluation by taking advantages of distilled auxiliary samples are conducted to demonstrate the generality ability of our method. The details about evaluation settings, datasets, architectures, and implementations will be discussed in the following subsections.

4.1 Evaluation Settings

We employ two evaluation settings, *i.e.*, inner-database evaluation, and cross-database evaluation.

Inner-database evaluation In Inner-database evaluation, the training set and test set are from the same database. For

example, if we conduct an inner-evaluation on RAF-DB 2.0, we use RAF-DB 2.0 training set and constructed dataset to train the FER learner, and then use the trained learner for evaluating the RAF-DB 2.0 test set.

Cross-database evaluation In Cross-dataset evaluation, the training set and test set are from different databases. For example, one of our cross-database evaluation settings is as follows: the training set is from RAF-DB 2.0 and constructed dataset, while the testing set is from CK+.

4.2 Databases

Experiments are conducted on five datasets, including Real-world Affective Face Database (RAF-DB) 2.0 [39], FER-2013 [40], Extended CohnKanade (CK+) [1], Japanese Female Facial Expression (JAFFE) [15], and MMI [14]. Auxiliary samples are selected from MS1M [41], which does not have any expression labels and therefore is considered as an unlabeled database.

RAF-DB 2.0 [39] contains 29,672 facial images which are collected from the Internet. It is a real-world database consisting of highly diverse samples. To achieve reliable labels for those samples, manually crowd-sourced annotation is conducted in [39]. There are two emotion sets in this dataset, *i.e.*, the basic expression label set, and the compound emotion label set. In this article, we focus on recognizing the basic expressions, and therefore we only utilize the basic expression label set, where there are 15,339 images divided into a training set (12,271 images) and a test set (3,068 images). To save the space, we use RAF-DB to denote RAF-DB 2.0 dataset in our discussion.

FER-2013 [40] was constructed for the ICML 2013 Challenges in Representation Learning, which contains 28,709 training images, 3,589 validation images, and 3,589 test images with basic expression labels. After being collected from the Internet automatically by Google search engine, all images are aligned and resized to 48×48 pixels.

CK+ [1] is a laboratory-controlled database that has been widely used in previous works for FER, where there are 593 video sequences collected from 123 subjects. In each sequence, there is a shift from a neutral expression in the first frame to the peak expression in the last frame. Among the 593 video sequences, there are 327 sequences labeled with basic expressions based on the Facial Action Coding System (FACS). Since CK+ does not provide official training/validation/test sets split, to make a fair comparison, we follow the setting in the previous work [19] to prepare the data. Specifically, first, we utilize the first frame as the neutral face of each labeled sequence and the last three peak frames with corresponding labels, resulting 1,308 images in total. Then the 1,308 images are divided into 10 groups for n-fold cross-validation experiments.

MMI [14] is constructed in a lab controlled environment, where there are 326 sequences in total, among which 213 sequences have basic expressions labels. Different from CK+, MMI is onset-apex-offset labeled, where the sequence in MMI begins with a neutral expression, reaches the peak expression in the middle, and then returns to a neutral expression. Pointed out by [27], the subjects in MMI might perform the same expression in different ways, and occlusions, *e.g.*, glasses, mustache, exist in some of the subjects.

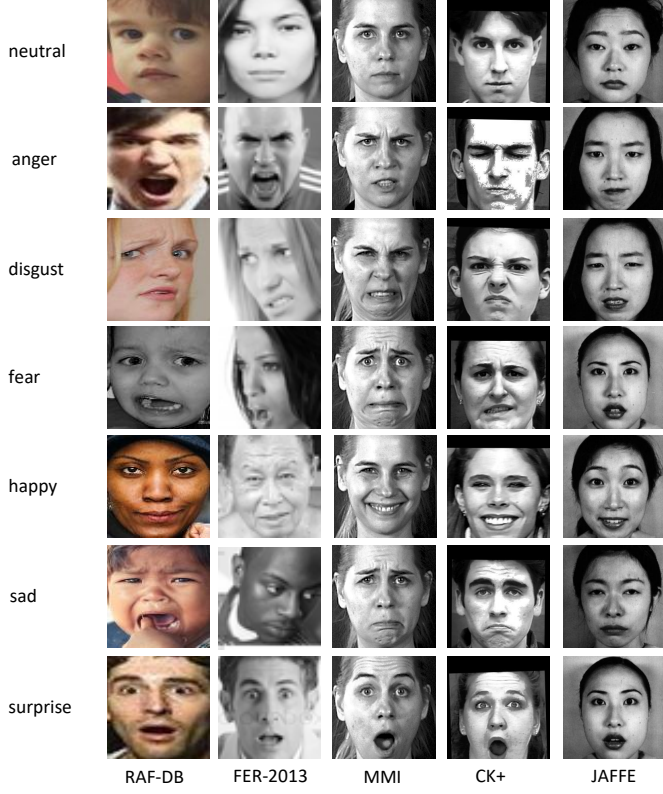


Fig. 2. Visualizing examples from databases utilized in this article. From top to bottom: neutral, anger, disgust, fear, happy, sad, and surprise. From left to right: RAF-DB 2.0, FER-2013, MMI, CK+, and JAFFE. Best viewed in color.

JAFFE [15] is a laboratory-controlled database containing 213 samples from 10 Japanese females, where each subject performs basic expressions 3 or 4 times. Due to the limited number of samples in this database, we utilize a leave-one-subject-out experimental setting.

MS-Celeb-1M(MS1M) [41] is a benchmark for the celebrity recognition. All images in MS1M are collected from the Internet. In version 1 of this dataset, there are around ten million images of one million celebrities captured in real scenarios. Due to its huge scale and variations, MS1M becomes one of the most challenging datasets for face recognition and face verification. We utilize the data provided on <https://github.com/ZhaoJ9014/face.evoLVe.PyTorch>.

There are 85,742 identities with 5,822,653 images in this pre-processed version, in which all the images are aligned by MTCNN [42] and resized to 112×112 . There is no expression label in this database, and therefore we can consider it as an unlabeled database in this work.

In Figure. 2, we show some example images from the databases utilized in this article. Those databases are collected in different scenarios, and therefore they have their own data bias. For example, 1) all faces in CK+ and JAFFE are frontal, while in RAF-DB, FER-2013, large face pose variations exist; 2) in FER-2013, CK+, and JAFFE, there is little color information to utilize; 3) the way to express “anger” in RAF-DB, FER-2013 are quite different from that in CK+ and JAFFE. We choose RAF-DB as the anchor database to select samples from MS1M, and use the selected samples to construct an auxiliary database for FER.

4.3 Implementation Details

In our experiments, we utilize two different architectures, *i.e.*, VGG-Face [33] and ResNet-34 [34], to test the efficiency and generality of our method. We choose those two architectures since they are the most frequently used networks in recent FER works [11], [32].

All the images utilized in our experiments are aligned by MTCNN [42] and resized to 224×224 . A data augmentation strategy of randomly horizontal flipping with 50% probability is utilized. During training, we utilize stochastic gradient descent with 0.9 momentum to optimize the network. The initial learning rate is set to 0.001, which will be multiplied by 0.1 every ten epochs. Unless noted, the total epoch number is set to 25. We implement the experiments by PyTorch [43] and run all settings on a workstation with four NVIDIA GTX 2080Ti GPU cards.

4.4 Performance Evaluation

This section verifies the efficacy of our method in both discriminative ability and generality capability. We conduct inner-database evaluation at first and then cross-dataset evaluation at second. The performance is evaluated by the mean classification accuracy.

4.4.1 Inner-dataset Evaluations

We conduct the inner-dataset evaluations on two in-the-wild databases, *i.e.*, RAF-DB, FER-2013 and one lab-controlled database, *i.e.*, CK+. We report the result comparisons with state-of-the-arts in Table.1, 2, and 3. RAF-DB is utilized as the anchor dataset for training the primitive learner. Auxiliary samples are selected from MS1M. To save the space, the auxiliary samples after data distillation are denoted as DAS (Distilled Auxiliary Samples), while the auxiliary samples before distillation are denoted as VAS (Vanilla Auxiliary Samples).

In Table. 1, we report our performance on RAF-DB. Based on Table. 1, we can find that by utilizing the auxiliary samples selected from MS1M, the proposed method outperforms the previous works. Specifically, compared to the previous work utilizing new loss functions [44], our method does not need any new loss functions. Comparing to [32] introducing more human labels into training, our method still outperforms it by almost 2% with few label cost. Since DAS is with a smaller size, its computation cost is much lower than VAS. The computation cost comparison is shown in Figure. 5. Although with much smaller training data, the performance of DAS is still comparable with the performance of VAS, which is 86.55% vs. 85.84% on VGG-Face, 85.24% vs. 85.84% on ResNet-34, respectively.

Table. 2 provides results on FER-2013. In this experimental setting, we test two anchor dataset cases, one is utilizing RAF-DB as the anchor dataset, and the other one is utilizing FER-2013 as the anchor dataset. From Table. 2, we can find that our method can achieve better or comparable results.

From Table. 1 and 2, we can find that: 1) VGG-Face network has better results than ResNet-34. We believe this is because VGG-Face is pretrained on a face recognition dataset while ResNet-34 is initialized on ImageNet, which makes VGG-Face more sensitive to face tasks. 2) distilled auxiliary samples achieve the best recognition accuracy in

both settings, *i.e.* 86.55% on RAF-DB and 73.27% on FER-2013, which demonstrates that the distilled images contain knowledge benefiting to the FER learner.

For CK+, we only conduct the experiment using VGG-Face and report the performance in Table. 3. Since the data size of CK+ is much smaller than the size of vanilla auxiliary data, we do not conduct the experiment on CK+ with vanilla auxiliary samples, but only report the accuracy using distilled auxiliary samples. In Table. 3, we can find that our method performs better than the baseline [32] and [20], or achieves comparable accuracy with much less label cost when comparing to [32].

4.4.2 Cross-dataset Evaluations

The cross-dataset evaluations and comparisons with previous state-of-the-arts are shown in Table. 4-7. Four datasets are used for test, which include: CK+, JAFFE, MMI, and FER-2013. We use the combination of RAF-DB and distilled auxiliary samples selected from MS1M as training set. We make a comparison with [16], which has the latest results on cross-dataset evaluation settings.

Based on experimental results in Table. 4-7, we can find that our method outperforms or achieves comparable results. We will give a more detailed analysis of the results for each dataset in the following paragraphs.

As shown in the Table. 4, our method achieves better performance than [16]. Unlike [16] using explicit domain adaptation strategy to minimize the domain gap between source dataset and target dataset, the better performance of our method is from the introduced distilled auxiliary samples with ignorable training cost.

The performance on JAFFE dataset is reported in Table. 5. As noted by [16], there is a high bias in this extremely small dataset, which has only 213 images. Due to this bias, the cross-dataset evaluation on JAFFE is comparatively lower than that on CK+. However, our method still outperforms [16].

As shown in Table. 6, for MMI dataset, our method achieves comparable accuracy with [16] with few computation cost, outperforms the baseline by a large margin, which is from 60.82% to 63.34%.

We also conduct a cross-dataset evaluation on FER-2013. FER-2013 was constructed for challenges and has huge variations introduced by expressive ways, head poses, scales, and etc. Due to the heavy variations existed in FER-2013, the performance under the cross-dataset setting is also inferior to that on CK+. In this challenging case, our method can still achieve a similar accuracy with [16] with seven distilled auxiliary samples.

4.4.3 Visualization

We visualize selected auxiliary examples from MS1M in Figure. 3, and the distilled auxiliary samples in Figure. 4. In total, our method select 117,369 auxiliary samples from MS1M.

Each row of Figure. 3 corresponds to one facial expressions. The images in each row are sorted by the distance between their feature and the nearest class centroid. Although there are large variations in MS1M, and a large domain gap between MS1M and the anchor dataset (RAF-DB), we can observe that the auxiliary samples selected



Fig. 3. Visualization of the selected auxiliary samples from MS1M database based on RAF-DB. Each row corresponds to one expression. The confidences of images in the same row are decreasing. Best viewed in color.

TABLE 1
Inner-dataset comparison of our method with previous works on RAF-DB. The performance of previous works are cited from [45].

Method	Accuracy (%)
FSN [46]	81.10
MRE-CNN [47]	82.63
baseDCNN [44]	82.66
DLP-CNN [44]	82.84
Center Loss [44]	82.86
PAT-VGG-F-(gender,race) [32]	83.83
PAT-ResNet-(gender,race) [32]	84.19
VGG-F (baseline)	85.15
ResNet-34 (baseline)	84.63
VAS + VGG-F (Ours)	85.84
VAS + ResNet-34 (Ours)	85.84
DAS + VGG-F (Ours)	86.55
DAS + ResNet-34 (Ours)	85.24

are still highly related to activated facial expression. From the images shown in Figure. 3, despite there are heavy illumination changes (the first column, second row), large poses (the first column and third column, sixth row), occlusions (fourth column, first row), our method still assigns correct expression labels for those samples. The high quality of those selected samples can explain why our method achieves a better performance after utilizing those auxiliary data.

Do the distilled auxiliary samples really contain underlying patterns? Based on the visualizations in Figure. 4, it is difficult to find any semantic meaning in them. All of the distilled images are full of specific texture patterns. This observation arouses us the question that whether those distilled images can provide useful knowledge for us. We conduct a simple experiment to test whether or not there

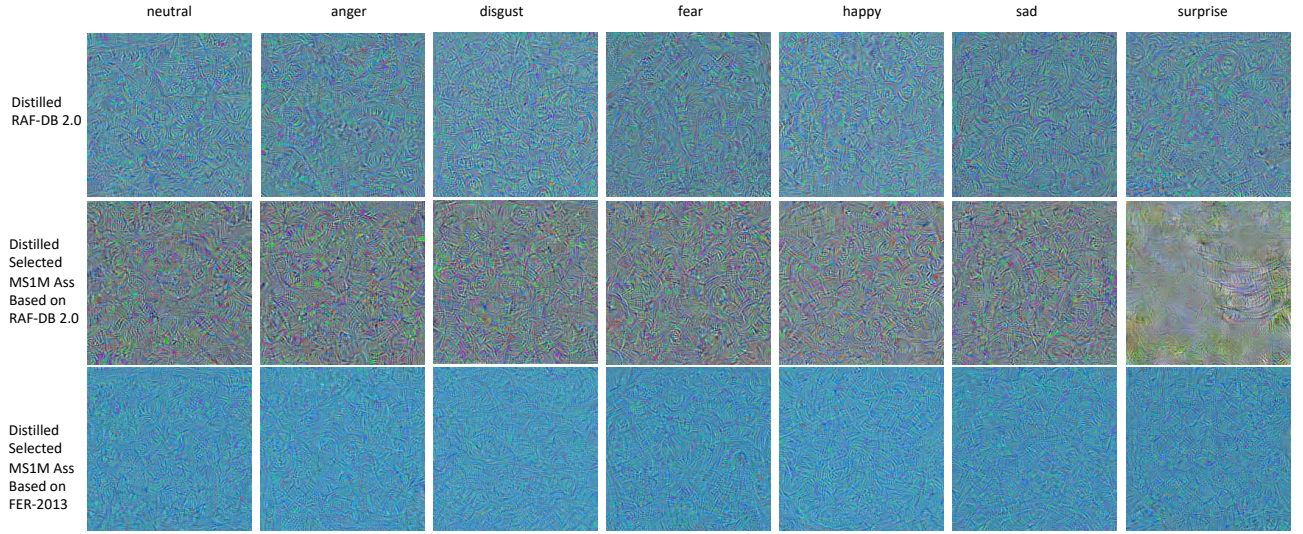


Fig. 4. Visualization of the distilled RAF-DB training set, distilled selected samples from MS1M database when using RAF-DB as anchor dataset, and distilled selected samples from MS1M when using FER-2013 as anchor dataset. Best viewed in color.

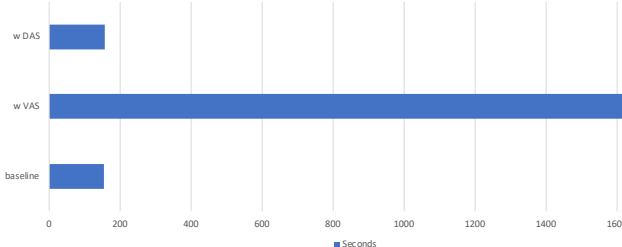


Fig. 5. Computation cost of without introducing auxiliary samples, with vanilla auxiliary samples, with distilled auxiliary samples. Best viewed in color.

TABLE 2

Inner-dataset comparison of our method with previous works on FER-2013. The performance of previous works are cited from [48].

Method	Accuracy (%)
ECNN [49]	69.96
DLSVM. [50]	71.2
Ron et al.. [51]	72.1
PAT-VGG-F-(gender,race). [32]	72.16
PAT-ResNet-(gender,race). [32]	72.00
VGG-F (baseline)	71.79
ResNet-34 (baseline)	70.89
RAF-DB as anchor database.	
VAS + VGG-F (Ours)	72.59
VAS + ResNet-34 (Ours)	70.31
DAS + VGG-F (Ours)	72.12
DAS + ResNet-34 (Ours)	71.23
FER-2013 as anchor database.	
VAS + VGG-F (Ours)	72.08
VAS + ResNet-34 (Ours)	70.98
DAS + VGG-F (Ours)	73.27
DAS + ResNet-34 (Ours)	71.20

are any underlying class related patterns in those distilled images. We save the intermediate distilled images in every ten epochs, resulting in 42 distilled images. We split them into a training set and testing set by a ratio of 5:1, and

TABLE 3
Inner-dataset comparison of our method with previous works on CK+. The performance of previous works are cited from [32].

Method	Accuracy (%)
Inception [20]	93.2
PAT-VGG-F-(gender,race) [32]	95.58
VGG-F (baseline) [32]	93.42
DAS + VGG-F (Ours)	95.35

TABLE 4
Cross-dataset comparison on CK+ dataset.

Method	Source	Target	Accuracy (%)
CNN-Li [16]	RAF-DB	CK+	78.00
VGG-F	RAF-DB+DAS	CK+	79.33

then feed the splitted training set and testing set to train a CNN. Our intuition is this: if those distilled auxiliary samples do not have any regular patterns corresponding to classes, then the CNN can not learn anything from them. What we observe is shown in Figure. 7. From this figure, we can find that the CNN trained on the distilled auxiliary samples converges very fast. The CNN can easily predict the images in the test set correctly, which indicates the existence of underlying patterns corresponding to different classes in each distilled sample.

Visualization of failure case. In Figure. 6, we visualize some failure cases by our method. As can be seen in this figure, some of them, *e.g.*, images in the first row, are misclassified due to huge head poses. The error introduced by large head poses can be solved by employing more advanced face alignment methods. For the images in the second row, poor lighting conditions make the network conduct incorrect predictions. In the third row, the occlusions on the face regions make them hard to recognize, some of them even for humans.

TABLE 5
Cross-dataset comparison on JAFFE dataset.

Method	Source	Target	Accuracy (%)
CNN-Li [16]	RAF-DB	JAFFE	54.26
VGG-F	RAF-DB+DAS	JAFFE	54.93

TABLE 6
Cross-dataset comparison on MMI dataset.

Method	Source	Target	Accuracy (%)
CNN-Li [16]	RAF-DB	MMI	64.13
VGG-F (baseline)	RAF-DB	MMI	60.82
VGG-F	RAF-DB+DAS	MMI	63.34



Fig. 6. Visualization of the failure case in RAF-DB test set. Best viewed in color.

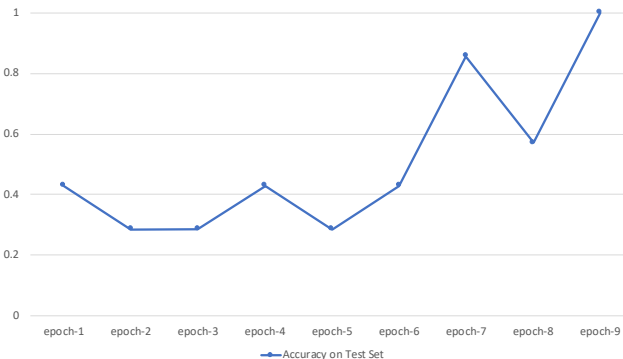


Fig. 7. Prediction curve of test set in distilled auxiliary samples. RAF-DB as the anchor dataset. Best viewed in color.

5 CONCLUSION

In this article, we propose a simple yet effective omni-supervised baseline for facial expression recognition. Unlike previous works using unlabeled data for pretraining, we exploit and distill the useful knowledge from a large-scale unlabeled data set constructed by our method, and enhance the FER performance. We have demonstrated that the distilled knowledge from the constructed large-scale unlabeled data has high generality by achieving significant advancement in inner-dataset and cross-dataset evaluations.

TABLE 7
Cross-dataset comparison on FER-2013 dataset.

Method	Source	Target	Accuracy (%)
CNN-Li [16]	RAF-DB	FER-2013	55.38
VGG-F	RAF-DB+DAS	FER-2013	55.17

REFERENCES

- P. Lucey, J. F. Cohn, T. Kanade, J. Saragih, Z. Ambadar, and I. Matthews, "The extended cohn-kanade dataset (ck+): A complete dataset for action unit and emotion-specified expression," in *CVPR-W*, 2010.
- Z. Zhang, M. Lyons, M. Schuster, and S. Akamatsu, "Comparison between geometry-based and gabor-wavelets-based facial expression recognition using multi-layer perceptron," in *FG*, 1998.
- Y. Zhang and Q. Ji, "Active and dynamic information fusion for facial expression understanding from image sequences," *IEEE Transactions on Pattern Analysis and Machine Intelligence*, 2005.
- Y.-l. Tian, T. Kanade, and J. F. Cohn, "Evaluation of gabor-wavelet-based facial action unit recognition in image sequences of increasing complexity," in *FG*, 2002.
- M. Eckhardt, I. Fasel, and J. Movellan, "Towards practical facial feature detection," *IJPRAI*, 2009.
- P. Yang, Q. Liu, and D. N. Metaxas, "Boosting coded dynamic features for facial action units and facial expression recognition," in *CVPR*, 2007.
- Y. Hu, Z. Zeng, L. Yin, X. Wei, X. Zhou, and T. S. Huang, "Multi-view facial expression recognition," in *FG*, 2008.
- M. Dahmane and J. Meunier, "Emotion recognition using dynamic grid-based hog features," in *FG*, 2011.
- T. Senechal, V. Rapp, H. Salam, R. Seguier, K. Bailly, and L. Prevost, "Combining aam coefficients with lgbp histograms in the multi-kernel svm framework to detect facial action units," in *FG*, 2011.
- M. F. Valstar, M. Mehu, B. Jiang, M. Pantic, and K. Scherer, "Meta-analysis of the first facial expression recognition challenge," *IEEE Transactions on Systems, Man, and Cybernetics, Part B (Cybernetics)*, 2012.
- Z. Meng, P. Liu, J. Cai, S. Han, and Y. Tong, "Identity-aware convolutional neural network for facial expression recognition," in *FG*, 2017.
- F. Zhang, T. Zhang, Q. Mao, and C. Xu, "Joint pose and expression modeling for facial expression recognition," in *CVPR*, 2018.
- H. Yang, U. Ciftci, and L. Yin, "Facial expression recognition by de-expression residue learning," in *CVPR*, 2018.
- M. Pantic, M. Valstar, R. Rademaker, and L. Maat, "Web-based database for facial expression analysis," in *ICME*, 2005.
- M. J. Lyons, S. Akamatsu, M. Kamachi, J. Gyoba, and J. Budynek, "The japanese female facial expression (jaffe) database," in *FG*, 1998.
- S. Li and W. Deng, "A Deeper Look at Facial Expression Dataset Bias," *IEEE Transactions on Affective Computing*, 2020.
- I. Radosavovic, P. Dollár, R. Girshick, G. Gkioxari, and K. He, "Data distillation: Towards omni-supervised learning," in *CVPR*, 2018.
- T. Wang, J.-Y. Zhu, A. Torralba, and A. A. Efros, "Dataset distillation," *arXiv preprint arXiv:1811.10959*, 2018.
- P. Liu, S. Han, Z. Meng, and Y. Tong, "Facial expression recognition via a boosted deep belief network," in *CVPR*, 2014.
- A. Mollahosseini, D. Chan, and M. H. Mahoor, "Going deeper in facial expression recognition using deep neural networks," in *WACV*, 2016.
- Y. Li, J. Zeng, S. Shan, and X. Chen, "Occlusion aware facial expression recognition using cnn with attention mechanism," *IEEE Transactions on Image Processing*, 2018.
- S. Zafeiriou and M. Petrou, "Sparse representations for facial expressions recognition via l1 optimization," in *CVPR-W*, 2010.
- Z.-L. Ying, Z.-W. Wang, and M.-W. Huang, "Facial expression recognition based on fusion of sparse representation," in *International Conference on Intelligent Computing*, 2010.
- P. Liu, S. Han, and Y. Tong, "Improving facial expression analysis using histograms of log-transformed nonnegative sparse representation with a spatial pyramid structure," in *FG*, 2013.
- L. Zhong, Q. Liu, P. Yang, B. Liu, J. Huang, and D. N. Metaxas, "Learning active facial patches for expression analysis," in *CVPR*, 2012.

- [26] B. Pan, S. Wang, and B. Xia, "Occluded facial expression recognition enhanced through privileged information," in *MM*, 2019.
- [27] L. Shan and D. Weihong, "Deep Facial expression recognition: A survey," *IEEE Transactions on Affective Computing*, 2020.
- [28] X. J. Zhu, "Semi-supervised learning literature survey," Tech. Rep., 2005.
- [29] A. Tarvainen and H. Valpola, "Mean teachers are better role models: Weight-averaged consistency targets improve semi-supervised deep learning results," in *NeurIPS*, 2017.
- [30] S. Laine and T. Aila, "Temporal ensembling for semi-supervised learning," in *ICLR*, 2017.
- [31] Y. Luo, R. Ji, T. Guan, J. Yu, P. Liu, and Y. Yang, "Every node counts: Self-ensembling graph convolutional networks for semi-supervised learning," *PR*, 2020.
- [32] J. Cai, Z. Meng, A. S. Khan, Z. Li, J. O'Reilly, and Y. Tong, "Probabilistic attribute tree in convolutional neural networks for facial expression recognition," *arXiv preprint arXiv:1812.07067*, 2018.
- [33] O. M. Parkhi, A. Vedaldi, and A. Zisserman, "Deep face recognition," in *BMVC*, 2015.
- [34] K. He, X. Zhang, S. Ren, and J. Sun, "Deep residual learning for image recognition," in *CVPR*, 2016.
- [35] J. Hu, L. Shen, and G. Sun, "Squeeze-and-excitation networks," in *CVPR*, 2018.
- [36] Y. Luo, P. Liu, T. Guan, J. Yu, and Y. Yang, "Significance-aware information bottleneck for domain adaptive semantic segmentation," in *ICCV*, 2019.
- [37] Y. Luo, L. Zheng, T. Guan, J. Yu, and Y. Yang, "Taking a closer look at domain shift: Category-level adversaries for semantics consistent domain adaptation," in *CVPR*, 2019.
- [38] Q. Zhang, J. Zhang, W. Liu, and D. Tao, "Category anchor-guided unsupervised domain adaptation for semantic segmentation," in *NeurIPS*, 2019.
- [39] S. Li and W. Deng, "Reliable crowdsourcing and deep locality-preserving learning for unconstrained facial expression recognition," *IEEE Transactions on Image Processing*, 2018.
- [40] I. J. Goodfellow, D. Erhan, P. L. Carrier, A. Courville, M. Mirza, B. Hamner, W. Cukierski, Y. Tang, D. Thaler, D.-H. Lee *et al.*, "Challenges in representation learning: A report on three machine learning contests," *Neural Networks*, 2015.
- [41] Y. Guo, L. Zhang, Y. Hu, X. He, and J. Gao, "Ms-celeb-1m: A dataset and benchmark for large-scale face recognition," in *ECCV*, 2016.
- [42] K. Zhang, Z. Zhang, Z. Li, and Y. Qiao, "Joint face detection and alignment using multitask cascaded convolutional networks," *IEEE Signal Processing Letters*, 2016.
- [43] A. Paszke, S. Gross, F. Massa, A. Lerer, J. Bradbury, G. Chanan, T. Killeen, Z. Lin, N. Gimelshein, L. Antiga, A. Desmaison, A. Kopf, E. Yang, Z. DeVito, M. Raison, A. Tejani, S. Chilamkurthy, B. Steiner, L. Fang, J. Bai, and S. Chintala, "Pytorch: An imperative style, high-performance deep learning library," in *NeurIPS*, 2019.
- [44] S. Li, W. Deng, and J. Du, "Reliable crowdsourcing and deep locality-preserving learning for expression recognition in the wild," in *CVPR*, 2017.
- [45] Z. Li, S. Han, A. S. Khan, J. Cai, Z. Meng, J. O'Reilly, and Y. Tong, "Pooling map adaptation in convolutional neural network for facial expression recognition," in *ICME*, 2019.
- [46] S. Zhao, H. Cai, H. Liu, J. Zhang, and S. Chen, "Feature selection mechanism in cnns for facial expression recognition," in *BMVC*, 2018.
- [47] Y. Fan, J. C. Lam, and V. O. Li, "Multi-region ensemble convolutional neural network for facial expression recognition," in *ICANN*, 2018.
- [48] J. Cai, "Improving person-independent facial expression recognition using deep learning," 2019.
- [49] G. Wen, Z. Hou, H. Li, D. Li, L. Jiang, and E. Xun, "Ensemble of deep neural networks with probability-based fusion for facial expression recognition," *Cognitive Computation*, 2017.
- [50] Y. Tang, "Deep learning using linear support vector machines," *arXiv preprint arXiv:1306.0239*, 2013.
- [51] R. Breuer and R. Kimmel, "A deep learning perspective on the origin of facial expressions," *arXiv preprint arXiv:1705.01842*, 2017.